ACKNOWLEDGMENTS

We are indebted to Dr. Messiah and Dr. Marshak for theoretical guidance, as we are to Dr. Kroll of Columbia University and to Professor Wentzel of Chicago. This research has been a group effort, and we are grateful to the members of our group, not primarily concerned with the work reported here, for many suggestions and much help. These men are Dr. M. L. Halbert and E. K. Gatchell, B. R. Grunstra, W. B. Johnson, P. P. Kane, and M. E. Nordberg, Jr.

PHYSICAL REVIEW VOLUME 99, NUMBER 3 AUGUST 1, 1955

L-Series X-Rays from π-Mesonic Atoms*†

M. CAMAC, M. L. HALBERT, AND J. B. PLATT
University of Rochester, Rochester, New York

(Received April 28, 1955)

The yields of the L-series x-ray lines from π-mesonic atoms have been measured for fourteen elements between $Z=6$ and 26. The total yield rises from 18% at carbon to a maximum of about 70% in the vicinity of aluminum, and then decreases. This decrease is caused primarily by nuclear absorption of pions from the $3d$ state; the $3d\rightarrow 2p$ yield determinations thus measure the nuclear absorption rate from the $3d$ state. The low-Z drop-off is predicted qualitatively by theoretical calculations of the meson cascade scheme. The observed relative intensities of the different L-series emission lines are substantially independent of Z in the range $6\leqq Z\leqq 16$. The $3d\rightarrow 2p$ transition energies are consistent with electromagnetically predicted values within the experimental error of 3 to 5% for $Z\leq 28$.

I. INTRODUCTION

THE x-ray emission lines from pi-mesonic atoms of light nuclei have been studied by Sterns, DeBenedetti, Stearns and Leipuner[1] and by Camac, McGuire, Platt, and Schulte.[2,3] Using the same equipment and similar techniques as the latter group we have measured the yield and the relative intensities of the L series for the elements $Z=6$ to 17 inclusive (except $Z=10$) and also $Z=20$, 22, and 26. These data furnish information on the competition between the $3d\rightarrow 2p$ radiative transition and the nuclear absorption of pions from the $3d$ state, and also on the cascade scheme of the mesonic atom. We have obtained energy measurements of the $3d\rightarrow 2p$ transitions for some of these elements, providing additional information on the specific pion-nucleus interaction.

The formation of the mesonic atom and details of the experimental procedure are described in the preceding article.[3] We proceed here with a discussion of the L-series data.

II. EXPERIMENTAL DATA

To illustrate the important features of the L-series data, we discuss in detail spectra obtained from several elements. We have chosen the spectra of oxygen, aluminum, and iron, shown in Figs. 1, 3, and 4. The vertical scales have been adjusted so that each spectrum is normalized to the same number of stopped mesons as the no-absorber spectrum for that element. The bars shown represent the standard deviation in a representative point.

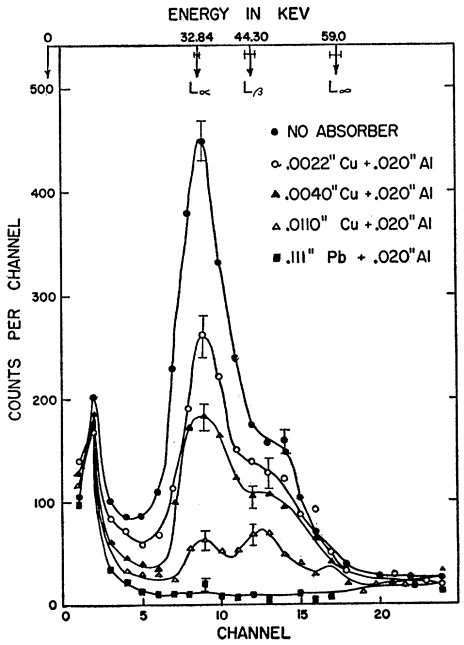

FIG. 1. Oxygen L series. Each spectrum was taken with the indicated x-ray absorber placed in front of the x-ray detector. The energy scale was determined by independent calibration with radioisotopes.

* This research was assisted by the U. S. Atomic Energy Commission.

† Based on a thesis submitted by M. L. Halbert to the Graduate School of the University of Rochester in partial fulfillment of the requirements for the degree of Doctor of Philosophy.

[1] Stearns, DeBenedetti, Stearns, and Leipuner, Phys. Rev. **93**, 1123 (1954).

[2] Camac, McGuire, Platt, and Schulte, Phys. Rev. **88**, 134 (1952); McGuire, Camac, Halbert, and Platt, Phys. Rev. **95**, 625 (1954).

[3] Camac, McGuire, Platt, and Schulte, preceding paper [Phys. Rev. **99**, 897 (1955)].

1. Oxygen, $Z=8$

Figure 1 shows spectra of photons observed in time coincidence with mesons stopping in a sample (H_2O) containing oxygen. These spectra were obtained with a NaI(Tl) scintillation counter and a 24-channel pulse-height analyzer and with the indicated x-ray absorbers between the H_2O sample and the x-ray detector. The energy scale shown was determined by independent calibration with the Ba x-rays from a Cs^{137} source. The arrows marking the predicted $L\alpha(3\rightarrow 2)$ and $L\beta(4\rightarrow 2)$ transition energies were located using the $3d\rightarrow 2p$ and $4d\rightarrow 2p$ energies calculated as described below in Sec. VI.

Above the L-series limit there are essentially no counts above the curve taken with the 0.111-inch lead absorber, which is practically opaque to x-rays of these energies. This plus the agreement of the observed with the predicted peak position we take as evidence that the main peak is the oxygen $L\alpha$ line. The existence of $L\beta$ and higher transitions is suggested by the structure of the high-energy side of the main peak in the no-absorber curve and is confirmed by the other spectra—the higher energy transitions are clearly attenuated less readily than the $L\alpha$ line. Each spectrum was separated into $L\alpha$, $L\beta$, and higher transitions. After subtraction of the 0.111-in. Pb background and correction for the 0.020-in. aluminum plate used to support the absorbers, the areas of the separated lines were plotted on semilogarithmic paper as a function of thickness of copper (Fig. 2). The lines on the graph, which seem to fit the points well, have slopes equal to the x-ray absorption coefficients in copper[4] at the predicted transition energies.

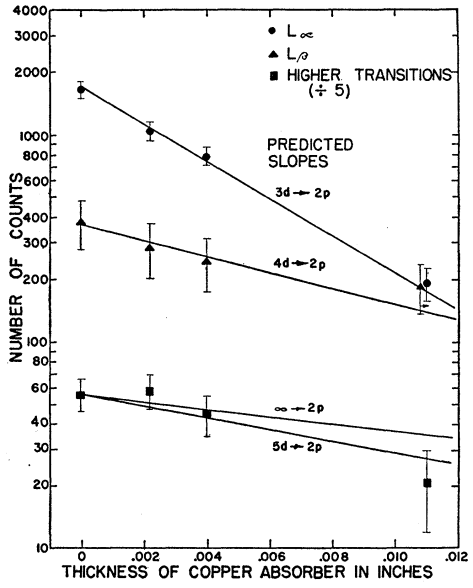

FIG. 2. Semilogarithmic plot of oxygen absorption data. The points are based on the spectra of Fig. 1; the lines are determined by the x-ray absorption coefficients at the various transition energies as given by Compton and Allison. To eliminate crowding, the data for the transitions higher than $L\beta$ have been divided by 5, and the 0.0110 in. point for $L\beta$ has been plotted at 0.0108 in.

The relative intensities of the various transitions obtained from the graph have to be corrected for absorption in the meson stopper. The lower-energy lines are attenuated more than the higher-energy transitions, making the latter appear more prominent in the spectra.

The peak in channel 2 cannot be due to low-energy x-rays because the opaque-absorber curve also shows it. The peak is instrumental, caused by nonlinearity in the the first three channels.

2. Aluminum, $Z=13$

In addition to the $L\beta$ and higher transitions, the aluminum L series (Fig. 3) shows structure on the low-energy side of the main peak as well. The iodine escape peak[5] for the $L\alpha$ line should be centered on channel 7; this accounts for the broadening of the main peak. The counts in the lower channels are probably due to the $n\rightarrow 3$ radiative transitions (M series). These become increasingly important as Z increases. However, the spectrum does not give an accurate measure of the M-series intensity because the energy threshold for x-ray detection was not low enough to include all of the M series.

The energy scale was determined by using the 72.1-kev Tl x-rays from an Hg^{203} source.

3. Iron, $Z=26$

The striking features of the iron L series (Fig. 4), namely the prominence of the M series and the relative smallness of the $L\alpha$ line, are typical of the L spectra of the elements of $Z\geqq 17$. An accurate determination of the L yield is therefore very difficult. The drop below channel 5 is due to electronic cut-off. The energy scale was determined with the 279-kev nuclear γ ray from an Hg^{203} source.

An absorber substantially opaque to the x-rays in this energy region was not used because it would have been inconveniently thick. Instead, we made use of a 0.030-in. tungsten absorber which should remove about 30% of the $L\alpha$ quanta. Dropping this curve in the vicinity of channel 15 by another 70% below the no-absorber spectrum gives an equivalent of the opaque-absorber curve. The dashed line suggests the result of such an operation. We believe the dashed line gives an absolute upper limit to the area of the peak. A lower limit which is probably closer to the true value is obtained by drawing a line under the observed peak which is tangent to the spectrum outside the region of the peak. In either case, the no-absorber spectrum is then poised above a substantial background, larger than that under the low-Z spectra because a much

[4] A. H. Compton and S. K. Allison, *X-Rays in Theory and Experiment* (D. Van Nostrand Company, Inc., New York, 1935), second edition, Appendix 9.

[5] P. Axel, Rev. Sci. Instr. **25**, 391 (1954).

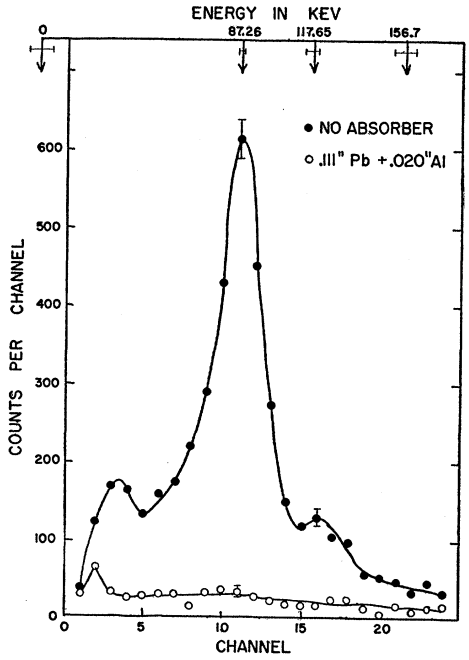

FIG. 3. Aluminum L series. Each spectrum was taken with the indicated x-ray absorber placed in front of the x-ray detector. The energy scale was determined by independent calibration with radioisotopes.

thicker NaI crystal had to be used for a reasonable detection efficiency at these energies.

III. CALCULATION OF YIELDS

We define the yield as the fraction of pions coming to rest in the stopper which give a mesonic x-ray of the desired type. In evaluating the L-series yields the problems encountered are somewhat different from those in the K-series case. We computed the L yields from a formula similar to that previously[3] used:

$$Y=\frac{N_x}{N_\pi \epsilon \bar{p}^* EK},$$

where N_x is the number of x-rays, N_π is the number of stopped pions, ϵ is the over-all efficiency of the x-ray detector (including the solid angle for detection), $\bar{p}^*$ is the effective photofraction, E is the escape correction, and K is the correction factor for photoabsorption and scattering. These quantities are discussed below.

Most of the factors in the formula are energy-dependent and vary appreciably over the energy range spanned by the L series. This necessitates computing the yield for each line of the L series separately. In practice, however, only the $L\alpha$ and $L\beta$ were treated separately; the higher transitions, because they cannot be individually resolved, were lumped together and the correction factors calculated for some energy between the $5\rightarrow 2$ and $\infty\rightarrow 2$ transition energies. The problems encountered in the L-yield calculations also differed from those met with in the K yields in that absorption of the L x-rays in a given stopper was more serious because L quanta are of much lower energy.

N_π, the observed number of stop events, included particles stopping in counter 3 as well as the stopper; the range curves tell what fraction actually came to rest in the stopper, usually between 85 and 95%. Large-angle scatterings in the stopper could have caused false stop events, but we have estimated that these constituted no more than a small fraction of a percent of the total. From the oxygen K spectra we learned that about 1% of the stopped particles give a μ x-ray.[3] We assumed the same is true for the L data and accordingly multiplied the number of stopped particles by 0.99 to arrive at the number of stopped pions. The 1% of the stopped particles which are muons make a negligible contribution to the L yield.

We used Teflon plastic (CF_2) and CCl_4 stoppers for the fluorine and chlorine data and assumed that these elements capture mesons in proportion to Z.[6] In a rough check of this "Z-law" we found that the number of carbon x-rays from CF_2 was 0.21 ± 0.11 of that from graphite, which is consistent with the Z-law prediction of 0.25.

N_x, the number of x-rays, was difficult to evaluate because of uncertainties in background and in how one

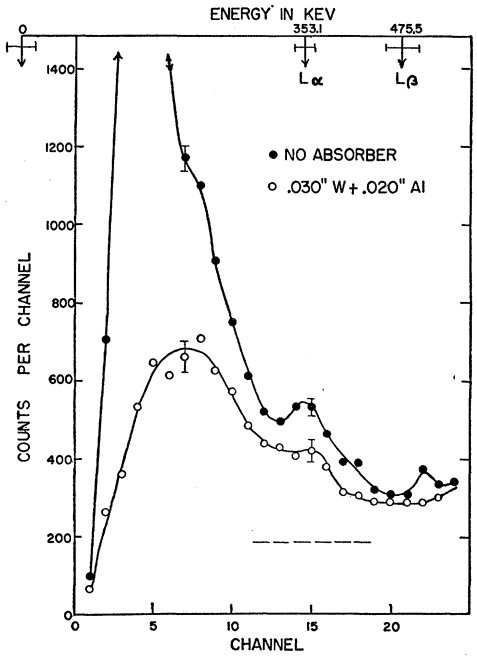

FIG. 4. Iron L series. Each spectrum was taken with the indicated x-ray absorber placed in front of the x-ray detector. The energy scale was determined by independent calibration with radioisotopes. The dashed line under the $L\alpha$ peak represents a lower limit to the background in that region. It was extrapolated from the observed attenuation of the 0.030 in. tungsten absorber.

[6] R. E. Marshak, *Meson Physics* (McGraw-Hill Book Company, Inc., New York, 1952), p. 170.

separates the individual lines of the L series. The curves taken with absorbers opaque or partially opaque to the L series determine only a lower limit to the background because any undesired γ rays of the same energy as the mesonic x-rays are also attenuated. The background counts are in time coincidence with stopped mesons. They probably result from stars following nuclear absorption of the pions. For $Z \leq 16$ the no-absorber curves approach the opaque-absorber curves in the regions where there are no mesonic x-rays (see Figs. 1 and 3), and we have taken the difference between the two as the observed number of x-rays.

For the elements $Z \geqq 17$, we could obtain only approximate upper and lower limits on the $L\alpha$ areas because of the presence of x-rays from the M series and the large background. The upper limit corresponds to identifying as the background the opaque-absorber spectrum (or its equivalent constructed from a partial-absorber curve as described above), and the lower limit to using only the area of the bump on the no-absorber spectrum at the $L\alpha$ energy. The treatment of the $L\beta$ and higher transitions was complicated even more by simultaneous detection of M and L quanta emitted in succession by a mesonic atom. Absorption evidence in the $Z=20$ spectrum is consistent with the apparent $L\beta$ peak being almost completely composed of pulses caused by detection of $L\alpha$ and $M\alpha$ quanta together; after correction for $M\alpha$ quanta we find the relative intensity of the $L\beta$ line is $7\% \pm 5\%$. For elements of $Z \geqq 20$ we have assumed for the yield calculations that none of the $L\beta$ or higher transitions are genuine; these counts have been grouped with the main $L\alpha$ peak. Fortunately the error in the total yield because of these uncertainties is far less than that due to the uncertainty in the background.

ϵ, the efficiency-solid angle product for x-ray detection averaged over the x-ray "source," was calculated by numerical integration, using the total γ-ray absorption coefficient in NaI at the energy of interest as given by White.[7] The average efficiency-solid angle product varied between 5 and 20%, depending on the energy and the geometry.

Corrections must be made for the x-ray interactions in the crystal which give a pulse smaller than that corresponding to the full energy. We calculated for our geometry the ratio p^* of the photopeak area to the area of the Compton continuum plus photopeak ("effective photo-fraction") from the data of Maeder, Müller, and Wintersteiger.[8] We corrected the separated L-line areas for escape of iodine K x-rays using Axel's calculations.[5] K is a correction factor needed because (a) not all of the mesonic x-rays initially directed toward the detector actually reached it—some were absorbed or scattered by the intervening material (stopper, counter 4, and the "window" of the NaI container), and (b) some mesonic x-rays not initially directed toward the detector were scattered into it by this material. We have estimated the factor K by supplementary experiments in which we measured the transmission of analogs of the stopper, counter 4, and the window for photons of various energies from radioisotope sources. For one set of $Z=6$ spectra the factor K for the $L\alpha$ line was only about 33%; above 40 kev it was always greater than 80%.

For most elements studied several independent sets of spectra were taken, often months apart; the yields calculated from these independent runs agree well. The final results listed in Table I are weighted averages of these separate determinations. The fractional errors are large for $Z=6$ and 7 because of uncertainty in the transmission factor K. For the other elements uncertainty in the L areas of the spectra is the most important. The purely statistical error is of relatively little significance.

TABLE I. Final results for total L-series yields and relative intensities.

Z	Total yield	$L\alpha$	$L\beta$	Higher transitions
6	0.18±0.06	0.79±0.28	0.13±0.03	0.08±0.02
7	0.25 0.06	0.73 0.14	0.17 0.05	0.10 0.03
8	0.34 0.03	0.70 0.10	0.17 0.05	0.13 0.03
9	0.37 0.09	0.78 0.13	0.16 0.07	0.13 0.03
11	0.64 0.05	0.78 0.07	0.12 0.03	0.10 0.03
12	0.50 0.04	0.79 0.10	0.13 0.04	0.08 0.01
13	0.68 0.06	0.77 0.08	0.12 0.04	0.11 0.01
14	0.75 0.11	0.75 0.08	0.15 0.03	0.10 0.03
15	0.52 0.14	0.73 0.13	0.13 0.03	0.14 0.03
16	0.59 0.14	0.73 0.08	0.13 0.05	0.14 0.03
17	0.46+0.08 −0.18			
20	0.31+0.08 −0.07			
22	0.16+0.17 −0.08			
26	0.12+0.26 −0.04			

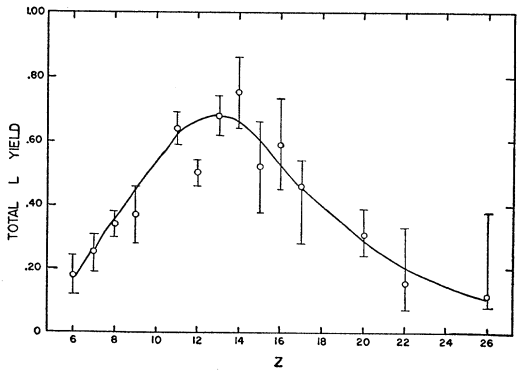

FIG. 5. Total L yield *vs* Z.

[7] G. R. White, National Bureau of Standards Report 1003, 1952 (unpublished).

[8] Maeder, Müller, and Wintersteiger, Helv. Phys. Acta **27**, 3 (1954).

IV. RELATIVE INTENSITIES

In Fig. 5 are plotted the total yield results of Table I. A smooth curve has been drawn through the points to emphasize the general trend. The point for $Z=12$ lies further off the curve than the estimated experimental error allows, but we feel this may be due to some accidental error. The error bars shown for $Z<17$ are the rms sums of the estimated errors in the various factors in the yield formula. For $Z\geq 17$ the errors introduced by background subtraction dominate. We believe the subtraction method used to determine the lower limit is closer to the correct procedure than that used for the upper limit and we have indicated with open circles our best estimate of the true yield value.

Measurements of the relative L yield have been published by the Carnegie group.[1] Allowing for the difference in the way background is subtracted (their procedure is equivalent to the method we used to find a lower limit on the areas), our results agree with theirs.

By relative intensity of a certain L transition we mean the number of such transitions occurring divided by the total number of all L transitions occurring. The relative intensities for the elements $Z\leqq 16$ are also listed in Table I. We have mentioned that $L\beta$ and higher transitions appear to be unimportant in the $Z\geqq 17$ elements; this is to be expected, for when the $n\rightarrow 3$ transitions go radiatively rather than by Auger emission a meson is more likely to be brought into the circular Bohr orbits. However, the experimental evidence is not reliable enough to allow us to assign these elements relative intensities for Table I.

V. NUCLEAR ABSORPTION FROM THE 3d STATE

A meson entering the $3d$ state will leave in either of two ways: (1) by a $3d\rightarrow 2p$ radiative transition ($L\alpha$), or (2) by direct nuclear absorption. (Auger transitions are unimportant for any elements we have studied; π-μ decay is also unimportant.) We denote the probability that a stopped meson enters the $3d$ state by P_{3d}, the $3d\rightarrow 2p$ radiative transition probability by W_r, and the probability of nuclear absorption by W_a. The yield $Y_{3d\rightarrow 2p}$ of $L\alpha$ quanta (not the total L yield) is thus given by

$$Y_{3d\rightarrow 2p}=P_{3d}W_r/(W_r+W_a).$$

We attribute the observed decrease in L yield at high Z to a more rapid increase with Z of W_a compared to W_r. This is theoretically expected from the following rough argument: Assuming hydrogen-like wave functions apply, $W_r\sim Z^4$ and $W_a\sim Z^8$; the latter dependence arises from multiplying the probability density near the origin for a d-state meson ($\sim Z^7$) by the number of particles in the nucleus which can absorb the meson ($\sim Z$).

We have plotted $1/Y_{3d\rightarrow 2p}$ against Z for $Z\geqq 11$ in Fig. 6. Solving the previous equation for W_a/W_r, we find

$$W_a/W_r=(P_{3d}/Y_{3d\rightarrow 2p})-1.$$

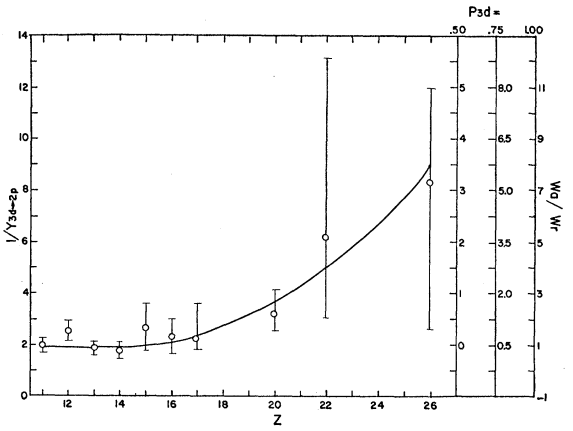

FIG. 6. Plot of $1/Y_{3d\rightarrow 2p}$ *vs* Z. The right-hand scales give the value of W_a/W_r implied by the data for three choices of P_{3d}.

Use of the right-hand scales of Fig. 6 performs this transformation automatically for three choices of P_{3d}. This parameter may depend on Z. P_{3d} can never be more than unity, and it cannot be much less than 0.5 for $Z=11$, 13, and 14 since W_a/W_r cannot become negative. The data for Z from 11 to 16 (except for $Z=12$) is consistent with $W_a/W_r=0$ if $P_{3d}\sim 0.5$; P_{3d} cannot be larger than 0.75 for these elements because of the observed relative intensity of the higher order transitions. On the other hand, the reduced relative intensity of the $L\beta$ and higher transitions for elements of $Z\geqq 20$ would imply that P_{3d} may be closer to 1 for these elements. The uncertainty in P_{3d} and in $L\alpha$ yield unfortunately make the data useful only for order-of-magnitude estimates of W_a/W_r. This is particularly true of $Z=26$, the most interesting element since it has the highest Z of any on which we have made yield measurements. For $Z=26$ W_a/W_r can be made to vary from 0.3 to 11.0 depending on the choice of assumptions.

VI. CASCADE SCHEME

If one knew the initial quantum states in which pions are captured in mesonic atoms, he could in principle predict the subsequent radiative and Auger transitions, and hence predict the quantum yield if only electromagnetic effects are important. Deviations from these predicted intensities would then give a direct determination of the competition from nuclear absorption. The distribution of pions following capture in states of high quantum numbers is not known; however one can assume various plausible distributions and attempt these yield predictions. We are currently making a study of these cascade schemes and expect to publish detailed results later; however some qualitative results may be of interest here.

TABLE II. Principal results of cascade calculations $Z=8$ and $Z=13$.

	$Z=8$ Population in $n=7$: equal	$2l+1$	l^2	$Z=13$ Population in $n=7$: equal	$2l+1$	l^2
(a) Relative intensity of						
$L\alpha$	0.54	0.63	0.71	0.53	0.62	0.71
$L\beta$	0.26	0.24	0.21	0.18	0.18	0.17
higher transitions	0.20	0.13	0.08	0.29	0.20	0.12
(b) Probability of L emission per meson in $n=7$	0.34	0.53	0.67	0.49	0.68	0.80

We have calculated tables of all important [i.e., $(n_1,l_1)\rightarrow(n_2,\ l_1\pm1)$] radiative and Auger[9,10] transition probabilities in oxygen ($Z=8$) and aluminum ($Z=13$) π-mesonic atoms for $n_1\leqq7$. These are based on the tabulations by Bethe[11] and Slack[12] of the radiative transition probabilities in the hydrogen atom, and a table provided by Dr. de Borde[13] of Auger rates assuming the electronic K and L shells are full. In these elements, for $n>7$, by far the most likely mechanism for meson energy loss is an Auger transition for which $\Delta n=-1$. Starting with various distributions of mesons in the $n=7$ states of these elements, their cascade down through the energy levels has been followed by use of these tables, noting the probability of radiative $n\rightarrow2$ transitions (L series). It was assumed that any meson entering an s state is removed from the cascade by nuclear absorption. Absorption from $l>0$ states was not taken into account.

Results of these calculations are given in Table II. The meson distribution in the various angular momentum states of $n=7$ were assumed to be weighted as l^2, $2l+1$, or equal weighting for each l.

The calculations of L-emission probability qualitatively predict a decrease in total L yield as Z changes from $Z=13$ to $Z=8$. This is observed experimentally. Detailed examination of the cascades shows that this is due to a greater tendency for mesons in oxygen atoms to bypass the $n=2$ states. The observed factor of two in total yield between the two elements is reproduced poorly by all of the $n=7$ populations, particullary the l^2 distribution. More detailed conclusions from comparison with experiment are unsafe because this calculated emission probability is not the same as the yield, but we can say that a uniform $n=7$ population for $Z=13$ appears to be ruled out since it gives an L-emission probability substantially less than the observed yield.

TABLE III. Observed and predicted $L\alpha$ transition energies and differences between observed and predicted energies, in kev.

Z	Observed	Predicted	Observed minus predicted
17	145± 8	149.8	−5± 8
22	251 6	252.2	−1± 6
26	357 14	353.1	+4±14
28	411 12	410.2	+1±12

The experimental data on $L\alpha$ relative intensity implies that an l^2 population is required in both elements. This in turn would imply an initial capture distribution even more sharply peaked toward large l values since for large n and l Auger transitions of the type $(n,l)\rightarrow(n-1,\ l-1)$ predominate, tending to preserve the initial l-distribution of the high l states above $n=7$.

VII. ENERGY MEASUREMENTS

Any deviation of the measured $3d\rightarrow2p$ transition energy from the energy predicted for this transition taking into account all significant electromagnetic effects should be due principally to shift of the $2p$ level caused by the specific pion-nucleus interaction. We have calculated the expected $3d\rightarrow2p$ energies using the Klein-Gordon solution for a point charge, corrected for reduced mass, vacuum polarization, finite extent of the nucleus, and nuclear polarization according to methods outlined by Grunstra[14] in his calculations of the $2p\rightarrow1s$ energies. The pion mass was taken as 273 electron masses; adjustment to the recent value[15] of 272.7 may be made by reducing the predicted energies by about 0.1%.

Measurements of the $L\alpha$ energy were made by comparison of the mesonic x-ray spectra with spectra of photons of known energy from radioisotopes, taken in alternate runs in the same geometry. The 279.2±0.2 kev[16] nuclear γ ray following β decay of Hg^{203} was the reference for the $Z=17$, 22 and 26 spectra; the 411.770 ±0.036 kev[17] γ ray following decay of Au^{198} was used for $Z=28$. Table III presents the results for these elements only. Any shift occurring should be more pronounced at high Z, but all observed energies agree with the predictions within the experimental error. The error is due principally to uncertainty in location of the center of the $L\alpha$ peak because of limited resolution and uncertain background.

[9] G. R. Burbidge and A. H. de Borde, Phys. Rev. **89**, 189 (1953).
[10] A. H. de Borde, Proc. Phys. Soc. (London) **A67**, 57 (1954).
[11] H. A. Bethe, *Handbuch der Physik* (Verlag Julius Springer, Berlin, 1933), second edition, Vol. **24**, Part 1, p. 444.
[12] F. G. Slack, table included at end of article by L. R. Maxwell, Phys. Rev. **38**, 1664 (1931).
[13] A. H. de Borde (private communication).
[14] B. R. Grunstra, thesis, University of Rochester, 1954 (unpublished).
[15] K. M. Crowe and R. H. Phillips, Phys. Rev. **96**, 470 (1954).
[16] A. H. Wapstra *et al.*, Proceedings of the 1954 Glasgow Conference, Pergamon Press, 1955.
[17] Muller, Hoyt, Klein, and DuMond, Phys. Rev. **88**, 775 (1952).

Fortunately it was on nickel ($Z=28$), the highest-Z element studied, that we could make the most precise energy measurement (partly because the calibration energy was practically equal to the $L\alpha$ energy). Attributing all the shift to the $2p$ level, we can say that the energy of the $2p$ state of $Z=28$ is affected by the specific pion-nucleus interaction no more than 12 kev, or 1.6%.

VIII. ACKNOWLEDGMENTS

The valuable assistance of E. K. Gatchell, B. R. Grunstra, W. B. Johnson, A. D. McGuire, and P. P. Kane in taking data, of E. C. Halbert and M. E. Mandl in performing calculations, and of the cyclotron crew, the shop personnel, and the engineering staff of the 130-inch Cyclotron Laboratory is gratefully acknowledged.

PHYSICAL REVIEW VOLUME 99, NUMBER 3 AUGUST 1, 1955

Energy of Electrons or Photons from Their Cascade Showers in Copper*

W. E. HAZEN
Ecole Polytechnique, Paris, France
(Received April 4, 1955)

The photographs obtained by the Ecole Polytechnique cloud-chamber group have been used for the study of cascade showers in copper plates produced by electrons of known momentum. The best constant for obtaining primary energy from the total number of track segments is given. The uncertainty in primary energy as determined by this method is found from the experimentally observed distributions. The results are applied to the interpretation of the heavy S-particle observed at the Massachusetts Institute of Technology.

1. INTRODUCTION

THE main interest in photon-electron cascade showers stems from their use as a tool. In the case of air showers, for example, one uses the theoretical results to estimate the energies of the incident primaries. In the case of particle interactions, one uses the shower-producing property as a qualitative means of identification of electrons or photons and tries to determine the energy from the size of the shower. Here we are dealing with showers in solids, in general, and, in the case of multiplate cloud chambers, the plate material is usually such that the available calculations are not very useful. The Monte-Carlo method[1] gives a better approximation than calculations but it is severely limited by the difficulty of handling the scattering problem. Thus, one must return to purely experimental results and use the theory for a guide or for minor corrections.

D'Andlau[2] has made a detailed study of the showers at particular depths with electron primaries of known energies. Among other things these results enable one to know the probability of mistaking an electron for a heavier particle when observing the penetrating power.

In the study of the radiation emitted by S-particles in multiplate cloud chambers, one is frequently faced with the question of estimating the energy of the initiators of electron-photon cascades.[3] Again, one must turn to experimental results. Previous work utilized π^0 mesons from nuclear disintegrations[3,4] but the statistics were not adequate to allow determination of a probability distribution.

The photographs of nuclear disintegrations obtained by the Ecole Polytechnique group[5] with their double cloud-chamber arrangement give the opportunity to observe the production of cascade showers by electrons of known momentum. Thus, one can observe the showers produced by electrons of known energy and from these data one can deduce the probability distribution in initiating energy for a shower of given size.

2. METHOD

(a) Selection of Data

The photographs of the lower chamber, which contained copper plates of one-centimeter thickness, were scanned for individual cascade showers. Showers that were selected were sufficiently distant from other events so that possible confusion with other radiation would only lead to uncertainties small compared with the inherent statistical uncertainty. The corresponding photographs of the upper chamber were inspected for cases in which the initiating particle could be identified unambiguously. Correspondence between tracks in the upper chamber and showers in the lower chamber could be determined to within $\sim$1 cm on the reprojection table of the laboratory. Since multiple scattering and

* This study was made while on leave from the University of Michigan as a Fulbright research scholar.

[1] R. R. Wilson, Phys. Rev. **86**, 261 (1952).

[2] C. A. D'Andlau, Nuovo cimento **12**, 859 (1954).

[3] Bridge, Courant, DeStaebler, and Rossi, Phys. Rev. **95**, 1101 (1954); H. Courant, Phys. Rev. **94**, 797(A) (1954).

[4] P. A. Bender, thesis, Washington University, St. Louis, Missouri, 1955 (unpublished).

[5] Gregory, Lagarrigue, Leprince-Ringuet, Muller, and Peyrou, Nuovo cimento **11**, 292 (1954).